

DOI: 10.1002/chem.201103028

4-(*N,N*-Dimethylamino)pyridine-Embedded Nanoporous Conjugated Polymer as a Highly Active Heterogeneous Organocatalyst

Yuan Zhang, Yong Zhang, Ya Lei Sun, Xin Du, Jiao Yi Shi, Wei David Wang, and Wei Wang*^[a]

Abstract: We report herein for the first time the incorporation of a versatile organocatalyst, 4-(*N,N*-dimethylamino)pyridine (DMAP), into the network of a nanoporous conjugated polymer (NCP) by the “bottom-up” approach. The resulting **DMAP-NCP** material possesses highly concentrated and homogeneously distributed DMAP catalytic sites (2.02 mmol g⁻¹). **DMAP-NCP** also exhibits enhanced stability and

permanent porosity due to the strong covalent linkage and the rigidity of the “bottom-up” monomers. As a result, **DMAP-NCP** shows excellent catalytic activity in the acylation of alcohols with yields of 92–99%. The **DMAP-**

NCP catalyst could be easily recovered from the reaction mixture and reused in at least 14 consecutive cycles without measurable loss of activity. Moreover, the catalytic acylation reaction could be performed under neat and continuous-flow conditions for at least 536 h of continuous work with the same catalyst activity.

Keywords: acylation • heterogeneous catalysis • nanoporous structures • organocatalysis • polymers

Introduction

In the past decade, organocatalysis^[1,2] has become a thriving area for the development of new concepts, robust organocatalysts, and efficient catalytic systems, as well as their widespread applications in synthetic organic chemistry, especially in pharmaceutical and natural product synthesis. The term organocatalysis applies solely to the use of (asymmetric) organic molecules, that is, metal-free organocatalysts, to realize a variety of reactions that were typically catalyzed by (transition) metal catalysts. Complementing metal and biocatalysis, organocatalysis possesses the advantages of non-toxicity, mild and robust procedures, as well as metal-free and readily available organocatalysts.^[2] However, most of the organocatalytic processes require high catalyst loading and rely on the tedious separation of the used organocatalyst from the product stream. Therefore, aiming at the easy purification of products and the recyclability of organocatalysts, the so-called “heterogeneous organocatalysis” has recently attracted increased attention.^[3] The methodology commonly used to prepare heterogeneous organocatalysts is the covalent immobilization of organocatalytic moieties onto certain solid supports by the “post-synthesis” approach.^[3] However, such “anchored” catalysts usually suffer

from several inherent flaws, for example, less and inhomogeneously distributed catalytic sites, poor stability, swelling, as well as mass transport issues.^[4] An attractive approach to possibly overcome these drawbacks is, therefore, the all-in-one construction of organocatalyst-embedded solid materials by the “bottom-up” strategy.^[5–7] This strategy allows the one-step synthesis of heterogeneous organocatalysts from organocatalytic monomers and structural linkers by means of condensation reactions, for example, olefin polymerization^[5,6] and cross-coupling reactions.^[7] By using this “bottom-up” approach, the organocatalytic sites can be homogeneously distributed within the polymeric frameworks and separated at controlled distances.^[7] In this regard, some pioneering work has recently been reported concerning the “bottom-up” construction of nonporous heterogeneous organocatalysts.^[5–7]

Very recently the “bottom-up” construction of functional porous solids (for example, periodic mesoporous organosilicas,^[8] metal organic frameworks (MOFs),^[9–11] and porous organic polymers^[12]) as heterogeneous catalysts has been attempted. In these cases, besides the embedding of catalytic moieties within the material network, the build-up of persistent porosity is the main concern within the “bottom-up” strategy. The micro- or mesopores formed by templating,^[8] intrinsic structural porosity,^[13] strong coordination,^[9–11] or rigidity of the building blocks^[14–22] would provide efficient access to the catalytic sites, thus facilitating the mass transport of reaction substrates and products.^[10b] In this context, however, the all-in-one construction of robust heterogeneous catalysts with both porosity and catalytic activity remains a challenging task.^[12] Moreover, very few^[11,21,22] examples of the one-step synthesis and catalytic application of porous organocatalysts can be found in the literature. For

[a] Dr. Y. Zhang, Y. Zhang, Y. L. Sun, Dr. X. Du, Dr. J. Y. Shi, W. D. Wang, Prof. Dr. W. Wang
State Key Laboratory of Applied Organic Chemistry
College of Chemistry and Chemical Engineering
Lanzhou University, Lanzhou, Gansu 730000 (P.R. China)
Fax: (+86)931-8915557
E-mail: wang_wei@lzu.edu.cn

Supporting information for this article is available on the WWW under <http://dx.doi.org/10.1002/chem.201103028>.

example, built from well-designed rigid monomers through strong covalent bonds, the recently discovered nanoporous conjugated polymers, that is, conjugated micro- and mesoporous polymers (CMPs),^[23] have received much research interest.^[24–26] Although new heterogeneous catalysts are therefore possible due to the advantages of tunable composition, permanent porosity, and good stability, only a few catalytic CMPs have been synthesized.^[15–20] Moreover, these catalytic CMPs are entirely concerned with metal catalysis,^[15–20] the “bottom-up” construction of CMPs as heterogeneous organocatalysts remains underdeveloped.^[22] Interestingly, covalent bonding, which is a characteristic of CMPs, should be more feasible for incorporating organocatalysts rather than metal-containing catalysts.

Motivated by the above-mentioned issues, in this contribution we report the “bottom-up” construction of a new nanoporous conjugated polymer (NCP), **DMAP-NCP** (Figure 1), which is a highly active and well recyclable hetero-

possibilities for the use of **DMAP-NCP** as a robust heterogeneous catalyst for industrial use.

Results and Discussion

Construction and characterization of DMAP-NCP: As depicted in Figure 1, **DMAP-NCP** could be reproducibly synthesized by palladium-catalyzed Sonogashira–Hagihara coupling^[28] of the functional monomer, 3,5-dibromo-*N,N*-dimethylpyridin-4-amine (**1**), and the structural linker, 1,3,5-triethynylbenzene (**2**), at 80 °C. After cooling, the resulting brown precipitate was filtered and washed several times with H₂O, ethanol, acetone, and chloroform followed by Soxhlet extraction using methanol at reflux. **DMAP-NCP** was then obtained as a brown powder after drying under vacuum at 60 °C. The **DMAP-NCP** polymer obtained is insoluble in all of the solvents tested and is stable up to 295 °C in air, as revealed by TGA (see Figure S1 in the Supporting Information). The morphology of **DMAP-NCP** was examined by SEM and TEM (Figures S2 and S3 in the Supporting Information). The SEM image shows that **DMAP-NCP** appears as loose aggregates of smaller particles with diameters ranging from 20 to 30 nm. Powder X-ray diffraction analysis revealed that **DMAP-NCP** is amorphous in nature (Figure S4 in the Supporting Information).

The permanent porosity of **DMAP-NCP** was investigated by nitrogen sorption measurements at 77 K (Figure 2). Figure 2a shows the nitrogen adsorption and desorption isotherms for **DMAP-NCP**. In accordance with the IUPAC classification,^[29] **DMAP-NCP** gives rise to Type IV nitrogen gas sorption isotherms with H2 hysteresis loops, which indicates that **DMAP-NCP** consists mainly of mesopores. The measured Brunauer–Emmett–Teller (BET) surface area of **DMAP-NCP** is 508 m² g⁻¹ and the total pore volume calculated from the amount of the N₂ gas adsorbed at $P/P_0=0.99$ is 0.46 cm³ g⁻¹. The micropore volume calculated by using the *t*-plot method is 0.05 cm³ g⁻¹. Accordingly, the calculated microporosity (micropore volume/total pore volume) is about 11 %, which also indicates that the **DMAP-NCP** network is mainly mesoporous.^[24d] The pore size distribution (PSD) for **DMAP-NCP**, as calculated by using nonlocal density functional theory (NLDFT), is shown in Figure 2b. The broad PSD curves suggest the coexistence of micro- and mesopores in **DMAP-NCP**. The micropores and small mesopores are formed mainly as a result of the rigidity of the building blocks, whereas large mesopores are most likely to arise from interparticle porosity.^[24g] The formation of a large number of mesopores could be attributed to the phase separation that occurs during the synthesis of the material.^[30] The relatively low reactivity of the dibromopyridine monomer **1** in the Sonogashira–Hagihara coupling reaction^[31] would cause this phase separation, which is consistent with previous observations.^[24g] The existence of massive mesopores may, therefore, facilitate the mass transport of reactants and products during the catalytic process.

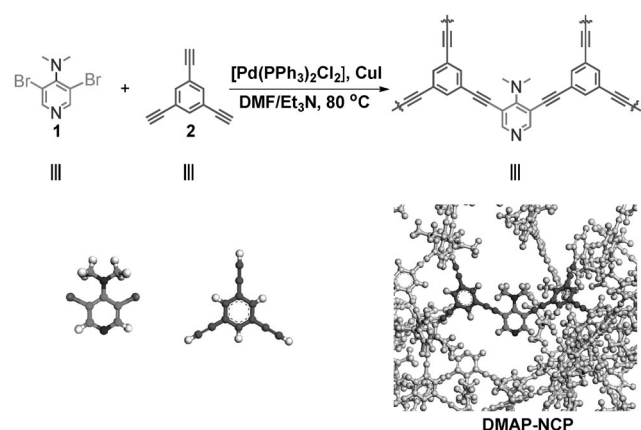


Figure 1. Construction of the DMAP-embedded nanoporous conjugated polymer (**DMAP-NCP**) by the “bottom-up” strategy. The functional monomer **1** and the structural linker **2** are connected through covalent bonds by the Sonogashira–Hagihara cross-coupling reaction. Highly concentrated and homogeneously distributed DMAP catalytic sites are therefore provided. Moreover, the nanopores (mainly mesopores) within **DMAP-NCP** provide efficient access to the catalytic sites, thus facilitating mass transport in heterogeneous organocatalysis.

ogeneous organocatalyst. The nanoporous **DMAP-NCP** polymer incorporates a high content (2.02 mmol g⁻¹) of an important organocatalyst, 4-(*N,N*-dimethylamino)pyridine (DMAP),^[27] within its framework. The nanoporous structure (mainly with mesopores), constructed by the Sonogashira–Hagihara coupling reaction of rigid building blocks **1** (functional DMAP monomer) and **2** (structural linker), should allow efficient mass transport. As a result, the nanoporous **DMAP-NCP** polymer shows excellent catalytic activity in the acylation of alcohols (yields of 92–99 %). The easily recycled **DMAP-NCP** catalyst could be reused for at least 14 cycles without measurable loss of activity. Moreover, the catalytic acylation reaction could be performed in neat (solvent-free) and continuous-flow conditions, which offers new

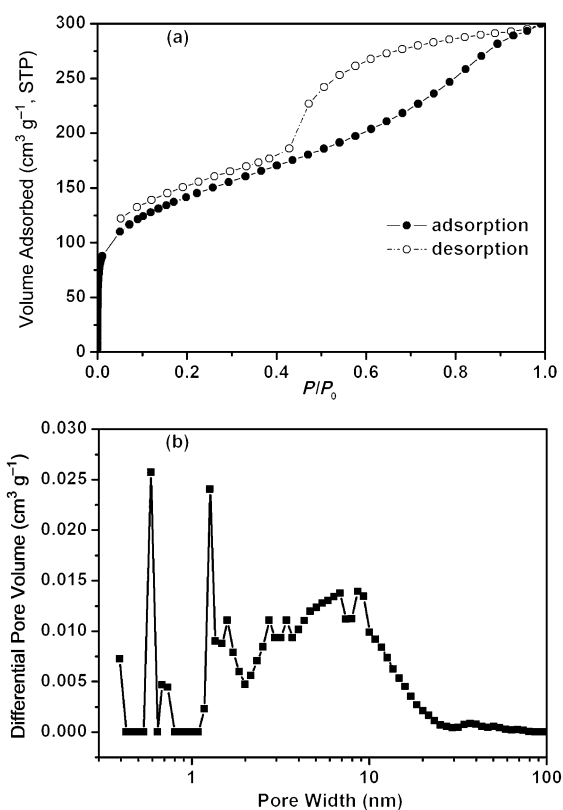


Figure 2. (a) Nitrogen adsorption–desorption isotherms for **DMAP-NCP** (STP=standard temperature and pressure). (b) Pore size distribution (PSD) for **DMAP-NCP**, calculated by nonlocal density functional theory (NLDFT).

The structure of **DMAP-NCP** at the atomic level was characterized by solid-state ^{13}C cross-polarization magic-angle spinning (CP/MAS) NMR spectroscopy. As shown in Figure 3, the peaks at around 153, 137, 116, and 44 ppm confirm the successful embedding of DMAP moieties within the **DMAP-NCP** network. The peaks at around 131 and

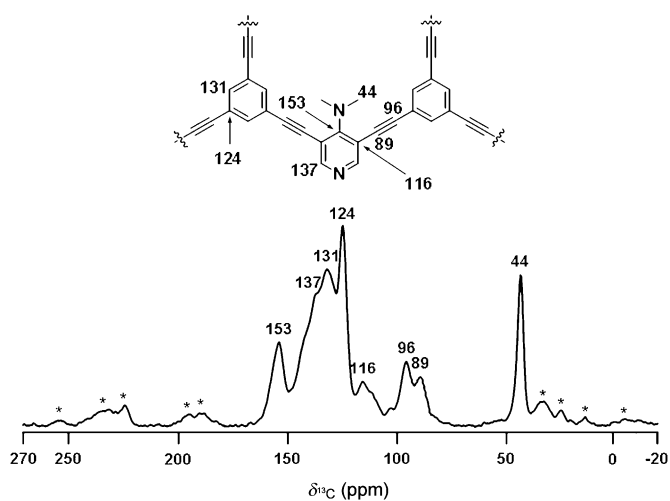


Figure 3. Solid-state ^{13}C CP/MAS NMR spectrum of **DMAP-NCP**. Asterisks denote spinning side-bands.

124 ppm correspond to the carbon atoms of $\text{C}_{\text{Ar-H}}$ and $\text{C}_{\text{Ar}}-\text{C}\equiv\text{C}-\text{C}_{\text{Ar}}$, respectively, which is consistent with the NMR assignments of previously synthesized CMP networks.^[24a,b] The peak assignments are illustrated in detail in Figure 3 (top). There is no evidence of peaks at around 76 and 82 ppm, which indicates that the $\text{C}\equiv\text{CH}$ groups are completely cross-coupled with **1** and that no homocoupling of 1,3,5-triethynylbenzene (**2**) occurs. Moreover, the peaks in the IR spectrum at around 1447 (corresponding to $\text{N}(\text{CH}_3)_2$ groups), 1517, and 1630 cm^{-1} (corresponding to the pyridine ring) also confirm that the DMAP skeleton is incorporated within the network of **DMAP-NCP** (see Figure S5 in the Supporting Information).

Catalytic performance of DMAP-NCP: As a versatile organocatalyst for promoting a variety of reactions, DMAP has been widely used in synthetic organic chemistry.^[32] Attempts to immobilize DMAP for heterogeneous organocatalysis have also been made.^[33] For example, Lin and co-workers^[33a] prepared a DMAP-functionalized mesoporous silica nanoparticle by the co-condensation method. McQuade and co-workers^[33b] reported a DMAP-modified linear polystyrene prepared by a copolymerization strategy. Gun'ko and Connon and their co-workers^[33c,d] developed the first magnetic nanoparticle-supported DMAP analogue. Legros and co-workers^[33e] synthesized a fluorosalt of DMAP as a recyclable catalyst. In contrast to the above methods, we constructed the DMAP-embedded nanoporous conjugated polymer **DMAP-NCP** by the “bottom-up” approach (Figure 1). Elemental analysis revealed that the synthesized **DMAP-NCP** contains extremely high densities of DMAP moieties (2.02 mmol g^{-1}) owing to the “bottom-up” approach of construction. The DMAP content in **DMAP-NCP** is much higher than those reported in DMAP-anchored catalysts. For example, in the magnetic nanoparticle-supported DMAP derivative, the DMAP content is only 0.20 mmol g^{-1} .^[33c] Therefore, in addition to the advantages of well-distributed DMAP catalytic sites and the nanoporous network, the use of **DMAP-NCP** as a catalyst should also be more desirable because the total amount of heterogeneous organocatalyst could be minimized.

The catalytic activity of **DMAP-NCP** was initially evaluated through the acylation reaction of 1-phenylethanol (**3**; Table 1). We were pleased to find that, upon treatment with 5 mol % of **DMAP-NCP** and 2.0 equiv of triethylamine in CH_2Cl_2 at ambient temperature (condition A), **3** underwent acylation to afford the acetyl derivative **4** almost quantitatively (Table 1, entry 1). Increasing the catalyst loading to 20 mol % (condition A) dramatically shortened the reaction time from 36 to 10 h (Table 1, entry 2). With a much higher catalytic activity than condition A, the catalytic acylation reaction could also be readily conducted in neat^[34] (solvent-free) conditions (condition B) without any external base to regenerate the catalyst into its neutral form. As shown in Table 1, entry 3, in the presence of 5 mol % of **DMAP-NCP**, **3** was quantitatively converted into acetyl derivative **4** within 10 h (condition B). This acylation reaction can also

Table 1. Optimization of the conditions for the acylation reaction.

Entry	Catalyst	Loading ^[a] [mol %]	Condition ^[b]	T [h]	Yield ^[c] [%]
1	DMAP-NCP	5	A	36	98
2	DMAP-NCP	20	A	10	98
3	DMAP-NCP	5	B	10	99
4	DMAP-NCP	1	B	48	97
6	no catalyst	--	B	10	trace
5	HCMP ^[d]	(20 mg)	B	10	trace

[a] Molar ratio of DMAP moieties relative to **3**: 20 mg of **DMAP-NCP** is approximately a loading of 20 mol % of DMAP moieties. [b] Condition A: **3** (0.2 mmol), Ac₂O (0.4 mmol), and NEt₃ (0.4 mmol) in dry CH₂Cl₂ (0.8 mL). Condition B: **3** (0.2 mmol) and Ac₂O (0.4 mmol) under neat conditions. [c] Isolated yield. [d] Obtained by the palladium-catalyzed homocoupling of 1,3,5-triethylbenzene (**2**), see ref.[35] for details.

be promoted with only 1 mol % of **DMAP-NCP** in neat conditions, although a longer reaction time of 48 h was required (Table 1, entry 4). In the absence of **DMAP-NCP**, or in the presence of **HCMP**^[35] without any DMAP sites, the acylation reaction scarcely proceeded and only trace amounts of the product were observed after 10 h (Table 1, entries 5 and 6). These control experiments demonstrated that the **DMAP-NCP** catalyst decisively contributes to the catalytic acylation reaction.

With these optimized conditions in hand, we then examined the substrate scope for this reaction (Table 2). We found that the acylation reactions of both aliphatic alcohols

Table 2. Acylation of alcohols and phenols catalyzed by **DMAP-NCP**.

Entry	Condition ^[a]	T [h]	Product	Yield ^[b] [%]
1	B	10		91
2	B	20		> 98
3	A	20		94
4	A	20		92
5	B	8		> 98
6	B	8		96
7	B	8		> 98

[a] Condition A: Alcohol (0.2 mmol), **DMAP-NCP** (20 mol %), and Ac₂O (2.0 equiv per hydroxy group), and NEt₃ (2.0 equiv per hydroxy group) in dry CH₂Cl₂ (0.8 mL) at RT. Condition B: Alcohol (0.2 mmol), **DMAP-NCP** (5 mol %), and Ac₂O (2.0 equiv) under neat conditions at RT. [b] Isolated yield.

(Table 2, entries 1–4) and phenols (Table 2, entries 5–7) with various substituent groups (electron-withdrawing, electron-donating, or bulky steric) were efficiently converted into the corresponding esters with excellent yields (92–99%) at ambient temperature. Notably, (–)-menthol, which has a relatively large steric hindrance, was quantitatively converted into the acetyl derivative even though an extended reaction time of 20 h was required (Table 2, entry 2). We also used **DMAP-NCP** to catalyze the ambient-temperature peracetylation of D-glucose (Table 2, entry 3) and D-mannitol (entry 4), which require the catalyst to mediate five and six separate acylation events per molecule, respectively; the reaction proceeded smoothly and the desired fully acetylated products were obtained in high yields (94 and 92%, respectively) within 20 h (Table 2, entries 3 and 4).

Next, we tested the recyclability and catalytic stability of the **DMAP-NCP** catalyst. The recycling experiments were performed with the acylation reaction of **3** under identical reaction conditions to those described in Table 1, entry 3. Separation of the product and recycling of the catalyst were easy. After the reaction, diethyl ether was added to dilute the reaction mixture and the organic layer was simply decanted after centrifugation to afford the desired products. The remaining catalyst was washed with further diethyl ether to remove any residual product and subjected to the next catalytic cycle. As shown in Figure 4, the **DMAP-NCP** catalyst

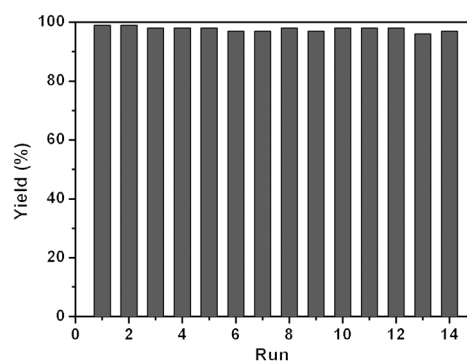


Figure 4. Evaluation of the recyclability of **DMAP-NCP** in the acylation reaction of 1-phenylethanol (**3**). All reactions were carried out with 4.0 mmol of **3** under identical reaction conditions to those described in Table 1, entry 3. The isolated yield is given.

can be reused for at least 14 iterative runs without measurable loss of activity. The ¹³C CP/MAS NMR spectrum of the catalyst recorded after the 14th run is almost identical to that of the fresh catalyst (see Figure S6 in the Supporting Information). Furthermore, nitrogen sorption experiments and elemental analysis revealed that the porosity of the used catalyst was well retained and that no DMAP moieties were leached during the catalytic processes. The recycled catalyst after the 14th run exhibited a BET surface area of 502 m² g⁻¹ and a catalyst loading of 1.95 mmol g⁻¹, which are almost identical to those of the fresh catalyst. These results not only illustrate the excellent stability and recyclability of the **DMAP-NCP** catalyst, but also imply that the mesopores

throughout the catalyst networks could provide efficient mass transport for the reactants and products.

In an effort to further demonstrate the persistent catalytic ability of **DMAP-NCP** and explore its potential for industrial use, we installed the **DMAP-NCP** catalyst in a column to conduct the catalytic acylation reaction under continuous-flow conditions^[36] (see the Supporting Information). The catalytic activity of the **DMAP-NCP** catalyst (Figure 5) did

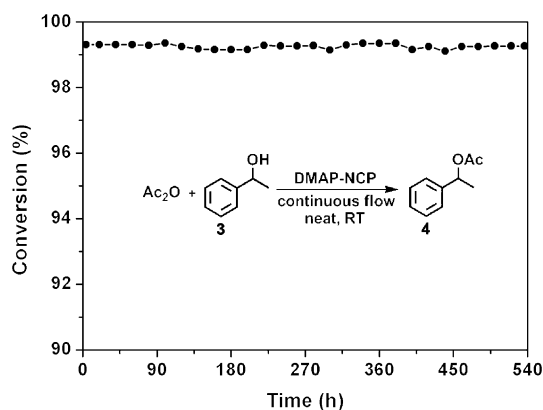


Figure 5. Catalytic performance of **DMAP-NCP** in the acylation of **3** under continuous-flow conditions (reaction column: 5.5 mm inner diameter and 15.1 cm length, 600 mg of **DMAP-NCP** catalyst; reaction conditions: a mixture of acetic anhydride and 1-phenylethanol (**3**) as the flow phase (2:1), flow rate = 0.2 mL h⁻¹, neat conditions, RT). The conversions were determined by GC analysis.

not reduce after 536 h of continuous work, which further indicates its superior persistent catalytic ability. Given its excellent stability and persistent catalytic ability as well as its straightforward synthesis, this organocatalytic **DMAP-NCP** porous polymer may, therefore, have potential practical applications in large-scale production.

We also demonstrated the catalytic utility of **DMAP-NCP** in the silylation of alcohols (see the Supporting Information). Primary alcohols were readily silylated in the presence of 20 mol % **DMAP-NCP**, affording the desired products in high yields. Moreover, **DMAP-NCP** promotes the selective silylation of primary alcohols (see the Supporting Information), which is very useful in organic synthesis.^[32d] These results further illustrate the generality of **DMAP-NCP** in catalyzing nucleophilic reactions.

Conclusion

We have demonstrated for the first time the successful incorporation of an important organocatalyst, DMAP, into the network of a nanoporous conjugated polymer by the “bottom-up” approach (Figure 1). The **DMAP-NCP** material we constructed possesses highly concentrated and homogeneously distributed catalytic sites, as well as enhanced stability. Moreover, the nanopores (mainly mesopores) of **DMAP-NCP** could facilitate the mass transport of reactants

and products during the catalytic reaction. As a result, the catalytic performance of the acylation of alcohols indicates that the **DMAP-NCP** catalyst possesses excellent catalytic activity. A variety of aliphatic alcohols and phenols could be effectively converted into the corresponding ester products in excellent yields (92–99%). Moreover, the catalytic activity did not show an appreciable decrease after 14 cycles, or after 536 h of continuous work, which illustrates the excellent stability and recyclability of the **DMAP-NCP** catalyst. Encouraged by these excellent catalytic results, which are among the best reported so far,^[33] we believe that **DMAP-NCP** may act as a promising heterogeneous catalyst in a variety of reactions catalyzed by DMAP (see the Supporting Information). Also, the persistent catalytic ability of **DMAP-NCP** under neat and continuous-flow conditions demonstrates its potential as a robust heterogeneous catalyst for industrial use. Furthermore, this study provides a new avenue for the heterogenization of other organocatalysts, especially of chiral organocatalysts.^[2] Research in this direction is underway in our laboratory.

Experimental Section

General methods: All reagents purchased from commercial sources were used as received. All solvents were purified and dried by standard methods prior to use. ¹H and ¹³C NMR spectra were recorded on a Bruker Avance 400 MHz spectrometer. Mass spectra were obtained on a Bruker Daltonics APEX II 47e FT-ICR mass spectrometer. ESI-MS spectra were recorded on a Bruker Daltonics esquire6000 mass spectrometer. Column chromatography was performed on silica gel (200–300 mesh). TLC was performed on silica gel GF254 plates.

Synthesis of DMAP-NCP: An oven-dried 25 mL Schlenk flask was charged with 1,3,5-triethynylbenzene (**2**; 300 mg, 2.0 mmol), 3,5-dibromo-*N,N*-dimethylpyridin-4-amine (**1**; 556 mg, 2.0 mmol), copper iodide (30 mg, 0.15 mmol), and bis(triphenylphosphine)palladium dichloride (70 mg, 0.1 mmol). Dry DMF (8.0 mL) and dry Et₃N (1.2 mL) were added to this flask under argon. The reaction mixture was heated at 80 °C for 72 h with stirring under argon. The mixture was then cooled to room temperature, the resulting brown precipitate was filtered and washed in turn (three times each) with water, ethanol, acetone, and chloroform. Further purification of the precipitate was carried out by Soxhlet extraction from methanol for 48 h to remove any unreacted monomer or catalyst residues. After drying in vacuum for 48 h at 60 °C, **DMAP-NCP** was obtained as a brown powder (542 mg, 102%). Elemental analysis calcd (%) for C₁₅H₁₀N₂: C 82.55, H 4.62, N 12.84; found: C 66.56, H 3.91, N 5.65. Found by energy-dispersive X-ray spectroscopy (EDX) analysis (wt. %): C 68.50, Br 21.08, Pd 3.76, Cu 2.51, I 2.18, P 1.97. The slightly higher (than expected) yield and the deviations in the elemental analysis can be attributed to the few unreacted bromopyridine end groups and the catalyst residues,^[24e] as identified by EDX (see Figure S7 in the Supporting Information).

General procedure for the DMAP-NCP-catalyzed acylation reactions: The alcohol of choice was dissolved in dry CH₂Cl₂ (if necessary) and then **DMAP-NCP**, triethylamine (if necessary), and acetic anhydride were added to the solution. The mixture was stirred at ambient temperature (for the reaction times, see Tables 1 and 2). After the reaction, diethyl ether (Et₂O) was added to dilute the reaction mixture and the catalyst was then isolated by centrifugation and thoroughly washed with Et₂O. The combined organic phase was evaporated under vacuum. The corresponding acetates were obtained by column chromatography with ethyl acetate/petroleum ether (16:1) as eluent. We conducted the following control experiments to demonstrate that the metal traces (Pd and Cu) in

the **DMAP-NCP** catalyst are not responsible for the catalytic acylation reactions: In the presence of [Pd(PPh₃)₂Cl₂] (0.25 mol%, the maximum possible Pd loading) and CuI (0.375 mol%, the maximum possible Cu loading) but absence of **DMAP-NCP**, the acylation reaction in Table 1 barely proceeded and only trace amounts of product were observed after 12 h.

Acknowledgements

This work was supported by the National Natural Science Foundation of China (No. 21172103), the Fundamental Research Funds for the Central Universities (No. lzujbky-2010-111), and the Youth Innovation Research Fund for Interdiscipline of Lanzhou University (No. LZUJC200912). We thank Mr. Jia Gao for his help in drawing the graphic illustration (Figure 1).

- [1] P. L. Dalko, L. Moisan, *Angew. Chem.* **2004**, *116*, 5248–5286; *Angew. Chem. Int. Ed.* **2004**, *43*, 5138–5175.
- [2] D. W. C. MacMillan, *Nature* **2008**, *455*, 304–308.
- [3] For reviews of recyclable organocatalysts, see: a) M. Benaglia, *New J. Chem.* **2006**, *30*, 1525–1533; b) F. Cozzi, *Adv. Synth. Catal.* **2006**, *348*, 1367–1390; c) M. Gruttadauria, F. Giacalone, R. Noto, *Chem. Soc. Rev.* **2008**, *37*, 1666–1688.
- [4] T. E. Kristensen, T. Hansen, *Eur. J. Org. Chem.* **2010**, 3179–3204.
- [5] a) T. E. Kristensen, K. Vestli, K. A. Fredriksen, F. K. Hansen, T. Hansen, *Org. Lett.* **2009**, *11*, 2968–2971; b) T. E. Kristensen, K. Vestli, M. G. Jakobsen, F. K. Hansen, T. Hansen, *J. Org. Chem.* **2010**, *75*, 1620–1629.
- [6] A. C. Evans, A. Lu, C. Ondeck, D. A. Longbottom, R. K. O'Reilly, *Macromolecules* **2010**, *43*, 6374–6380.
- [7] A. B. Powell, Y. Suzuki, M. Ueda, C. W. Bielawski, A. H. Cowley, *J. Am. Chem. Soc.* **2011**, *133*, 5218–5220.
- [8] A. Kuschel, S. Polarz, *J. Am. Chem. Soc.* **2010**, *132*, 6558–6565.
- [9] a) C. D. Wu, A. G. Hu, L. Zhang, W. B. Lin, *J. Am. Chem. Soc.* **2005**, *127*, 8940–8941; b) L. Q. Ma, J. M. Falkowski, C. Abney, W. B. Lin, *Nat. Chem.* **2010**, *2*, 838–846; c) F. Song, C. Wang, J. M. Falkowski, L. Ma, W. B. Lin, *J. Am. Chem. Soc.* **2010**, *132*, 15390–15398; d) C. Wang, Z. G. Xie, K. E. deKrafft, W. B. Lin, *J. Am. Chem. Soc.* **2011**, *133*, 13445–13454; e) K. Gedrich, M. Heitbaum, A. Notzon, I. Senkowska, R. Fröhlich, J. Getzschmann, U. Mueller, F. Glorius, S. Kaskel, *Chem. Eur. J.* **2011**, *17*, 2099–2106.
- [10] a) J. Y. Lee, O. K. Farha, J. Roberts, K. A. Scheidt, S. T. Nguyen, J. T. Hupp, *Chem. Soc. Rev.* **2009**, *38*, 1450–1459; b) L. Q. Ma, C. Abney, W. B. Lin, *Chem. Soc. Rev.* **2009**, *38*, 1248–1256.
- [11] For a recent example of organocatalytic MOFs, see: D. J. Lun, G. I. N. Waterhouse, S. G. Telfer, *J. Am. Chem. Soc.* **2011**, *133*, 5806–5809.
- [12] For a recent review on porous organic polymers in catalysis, see: P. Kaur, J. T. Hupp, S. T. Nguyen, *ACS Catal.* **2011**, *1*, 819–835.
- [13] a) P. M. Budd, B. Ghanem, K. Msayib, N. B. McKeown, C. Tattershall, *J. Mater. Chem.* **2003**, *13*, 2721–2726; b) H. J. Mackintosh, P. M. Budd, N. B. McKeown, *J. Mater. Chem.* **2008**, *18*, 573–578; c) S. Makhseed, F. Al-Kharafi, J. Samuel, B. Ateya, *Catal. Commun.* **2009**, *10*, 1284–1287.
- [14] a) Y. Zhang, S. N. Riduan, J. Y. Ying, *Chem. Eur. J.* **2009**, *15*, 1077–1081; b) R. Palkovits, M. Antonietti, P. Kuhn, A. Thomas, F. Schuth, *Angew. Chem.* **2009**, *121*, 7042–7045; *Angew. Chem. Int. Ed.* **2009**, *48*, 6909–6912; c) C. E. Chan-Thaw, A. Villa, P. Katekomol, D. Su, A. Thomas, L. Prati, *Nano Lett.* **2010**, *10*, 537–541; d) C. E. Chan-Thaw, A. Villa, L. Prati, A. Thomas, *Chem. Eur. J.* **2011**, *17*, 1052–1057.
- [15] X. Du, Y. L. Sun, B. E. Tan, Q. F. Teng, X. J. Yao, C. Y. Su, W. Wang, *Chem. Commun.* **2010**, *46*, 970–972.
- [16] L. Chen, Y. Yang, D. L. Jiang, *J. Am. Chem. Soc.* **2010**, *132*, 9138–9143.
- [17] A. M. Shultz, O. K. Farha, J. T. Hupp, S. T. Nguyen, *Chem. Sci.* **2011**, *2*, 686–689.
- [18] J. X. Jiang, C. Wang, A. Laybourn, T. Hasell, R. Clowes, Y. Z. Khimyak, J. L. Xiao, S. J. Higgins, D. J. Adams, A. I. Cooper, *Angew. Chem.* **2011**, *123*, 1104–1107; *Angew. Chem. Int. Ed.* **2011**, *50*, 1072–1075.
- [19] Z. G. Xie, C. Wang, K. E. deKrafft, W. B. Lin, *J. Am. Chem. Soc.* **2011**, *133*, 2056–2059.
- [20] L. Q. Ma, M. M. Wanderley, W. B. Lin, *ACS Catal.* **2011**, *1*, 691–697.
- [21] M. Rose, A. Notzon, M. Heitbaum, G. Nickerl, S. Paasch, E. Brunner, F. Glorius, S. Kaskel, *Chem. Commun.* **2011**, *47*, 4814–4816.
- [22] H. C. Cho, H. S. Lee, J. Chun, S. M. Lee, H. J. Kim, S. U. Son, *Chem. Commun.* **2011**, *47*, 917–919.
- [23] For excellent reviews on porous organic polymer networks, see: a) A. I. Cooper, *Adv. Mater.* **2009**, *21*, 1291; b) A. Thomas, P. Kuhn, J. Weber, M.-M. Titirici, M. Antonietti, *Macromol. Rapid Commun.* **2009**, *30*, 221–236; c) J. Germain, J. M. J. Frechet, F. Svec, *Small* **2009**, *5*, 1098–1111; d) N. B. McKeown, P. M. Budd, *Macromolecules* **2010**, *43*, 5163–5176; e) J. X. Jiang, A. I. Cooper, *Top. Curr. Chem.* **2010**, *293*, 1–33; f) A. Thomas, *Angew. Chem.* **2010**, *122*, 8506–8523; *Angew. Chem. Int. Ed.* **2010**, *49*, 8328–8344.
- [24] a) J. X. Jiang, F. Su, A. Trewin, C. D. Wood, N. L. Campbell, H. Niu, C. Dickinson, A. Y. Ganin, M. J. Rosseinsky, Y. Z. Khimyak, A. I. Cooper, *Angew. Chem.* **2007**, *119*, 8728–8732; *Angew. Chem. Int. Ed.* **2007**, *46*, 8574–8578; b) J. X. Jiang, F. Su, A. Trewin, C. D. Wood, H. Niu, J. T. A. Jones, Y. Z. Khimyak, A. I. Cooper, *J. Am. Chem. Soc.* **2008**, *130*, 7710–7720; c) J. X. Jiang, F. Su, H. Niu, C. D. Wood, N. L. Campbell, Y. Z. Khimyak, A. I. Cooper, *Chem. Commun.* **2008**, 486–488; d) R. Dawson, F. Su, H. Niu, C. D. Wood, J. T. A. Jones, Y. Z. Khimyak, A. I. Cooper, *Macromolecules* **2008**, *41*, 1591–1593; e) E. Stöckel, X. F. Wu, A. Trewin, C. D. Wood, R. Clowes, N. L. Campbell, J. T. A. Jones, Y. Z. Khimyak, D. J. Adams, A. I. Cooper, *Chem. Commun.* **2009**, 212–214; f) J. X. Jiang, A. Trewin, F. Su, C. D. Wood, H. Niu, J. T. A. Jones, Y. Z. Khimyak, A. I. Cooper, *Macromolecules* **2009**, *42*, 2658–2666; g) R. Dawson, A. Laybourn, R. Clowes, Y. Z. Khimyak, D. J. Adams, A. I. Cooper, *Macromolecules* **2009**, *42*, 8809–8816; h) A. Trewin, A. I. Cooper, *Angew. Chem.* **2010**, *122*, 1575–1577; *Angew. Chem. Int. Ed.* **2010**, *49*, 1533–1535; i) T. Hasell, C. D. Wood, R. Clowes, J. T. A. Jones, Y. Z. Khimyak, D. J. Adams, A. I. Cooper, *Chem. Mater.* **2010**, *22*, 557–564; j) J. X. Jiang, A. Trewin, D. J. Adams, A. I. Cooper, *Chem. Sci.* **2011**, *2*, 1777–1781.
- [25] a) P. Kuhn, M. Antonietti, A. Thomas, *Angew. Chem.* **2008**, *120*, 3499–3502; *Angew. Chem. Int. Ed.* **2008**, *47*, 3450–3453; b) P. Kuhn, A. Forget, D. S. Su, A. Thomas, M. Antonietti, *J. Am. Chem. Soc.* **2008**, *130*, 13333–13337; c) P. Kuhn, A. Thomas, M. Antonietti, *Macromolecules* **2009**, *42*, 319–326; d) J. Weber, A. Thomas, *J. Am. Chem. Soc.* **2008**, *130*, 6334–6335; e) J. Schmidt, M. Werner, A. Thomas, *Macromolecules* **2009**, *42*, 4426–4429; f) J. Schmidt, J. Weber, J. D. Epping, M. Antonietti, A. Thomas, *Adv. Mater.* **2009**, *21*, 702–705; g) M. G. Schwab, B. Fassbender, H. W. Spiess, A. Thomas, X. L. Feng, K. Mullen, *J. Am. Chem. Soc.* **2009**, *131*, 7216–7217.
- [26] a) M. Rose, W. Bohlmann, M. Sabo, S. Kaskel, *Chem. Commun.* **2008**, 2462–2464; b) O. K. Farha, A. M. Spokoynny, B. G. Hauser, Y.-S. Bae, S. E. Brown, R. Q. Snurr, C. A. Mirkin, J. T. Hupp, *Chem. Mater.* **2009**, *21*, 3033–3035; c) T. Ben, H. Ren, S. Q. Ma, D. P. Cao, J. H. Lan, X. F. Jing, W. C. Wang, J. Xu, F. Deng, J. M. Simmons, S. L. Qiu, G. S. Zhu, *Angew. Chem.* **2009**, *121*, 9621–9624; *Angew. Chem. Int. Ed.* **2009**, *48*, 9457–9460; d) S. W. Yuan, B. Dorney, D. White, S. Kirklín, P. Zapol, L. P. Yu, D. J. Liu, *Chem. Commun.* **2010**, *46*, 4547–4549; e) L. Chen, Y. Honsho, S. Seki, D. Jiang, *J. Am. Chem. Soc.* **2010**, *132*, 6742–6748; f) Q. Chen, M. Luo, T. Wang, J. X. Wang, D. Zhou, Y. Han, C. S. Zhang, C. G. Yan, B. H. Han, *Macromolecules* **2011**, *44*, 5573–5577.
- [27] W. Steglich, G. Höfle, *Angew. Chem.* **1969**, *81*, 1001–1001; *Angew. Chem. Int. Ed. Engl.* **1969**, *8*, 981–981.
- [28] K. Sonogashira, Y. Tohda, N. Hagihara, *Tetrahedron Lett.* **1975**, *16*, 4467–4470.

- [29] K. S. W. Sing, D. H. Everett, R. A. W. Haul, L. Moscou, R. A. Pierotti, J. Rouquerol, T. Siemieniowska, *Pure Appl. Chem.* **1985**, *57*, 603–619.
- [30] D. C. Sherrington, *Chem. Commun.* **1998**, 2275–2286.
- [31] R. Chinchilla, C. Nájera, *Chem. Rev.* **2007**, *107*, 874–922.
- [32] For reviews on the use of DMAP in catalysis, see: a) A. C. Spivey, S. Arseniyadis, *Angew. Chem.* **2004**, *116*, 5552–5557; *Angew. Chem. Int. Ed.* **2004**, *43*, 5436–5441; b) R. Murugan, E. F. V. Scriven, *Aldrichimica Acta* **2003**, *36*, 21–29; c) U. Ragnarsson, L. Grehn, *Acc. Chem. Res.* **1998**, *31*, 494–501; d) E. F. V. Scriven, *Chem. Soc. Rev.* **1983**, *12*, 129–161; e) G. Höfle, W. Steglich, H. Vorbruggen, *Angew. Chem.* **1978**, *90*, 602–615; *Angew. Chem. Int. Ed. Engl.* **1978**, *17*, 569–583.
- [33] For selected examples of recyclable DMAP derivatives in catalysis, see: a) H.-T. Chen, S. Huh, J. W. Wiench, M. Pruski, V. S.-Y. Lin, *J. Am. Chem. Soc.* **2005**, *127*, 13305–13311; b) K. E. Price, B. P. Mason, A. R. Bogdan, S. J. Broadwater, J. L. Steinbacher, D. T. McQuade, *J. Am. Chem. Soc.* **2006**, *128*, 10376–10377; c) C. Ó. Dálaigh, S. A. Corr, Y. Gun'ko, S. J. Connon, *Angew. Chem.* **2007**, *119*, 4407–4410; *Angew. Chem. Int. Ed.* **2007**, *46*, 4329–4332; d) O. Gleeson, R. Tekoriute, Y. Gun'ko, S. J. Connon, *Chem. Eur. J.* **2009**, *15*, 5669–5673; e) D. Vuluga, J. Legros, B. Crousse, D. Bonnet-Delpon, *Chem. Eur. J.* **2010**, *16*, 1776–1779; f) I. Pulko, J. Wall, P. Krajnc, N. R. Cameron, *Chem. Eur. J.* **2010**, *16*, 2350–2354; g) A. Corma, H. Garcia, A. Leyva, *Chem. Commun.* **2003**, 2806–2807; h) F. M. Menger, D. J. McCann, *J. Org. Chem.* **1985**, *50*, 3928–3930; i) S. Shinkai, H. Tsuji, Y. Hara, O. Manabe, *Bull. Chem. Soc. Jpn.* **1981**, *54*, 631–632; j) D. E. Bergbreiter, P. L. Osburn, C. M. Li, *Org. Lett.* **2002**, *4*, 737–740; k) E. J. Delaney, L. E. Wood, I. M. Klotz, *J. Am. Chem. Soc.* **1982**, *104*, 799–807.
- [34] A. Sakakura, K. Kawajiri, T. Ohkubo, Y. Kosugi, K. Ishihara, *J. Am. Chem. Soc.* **2007**, *129*, 14775–14779.
- [35] **HCMP** stands for “homocoupled conjugated microporous polymer”, a type of porous organic polymer reported by Cooper et al.^[24c] that was produced by the palladium-catalyzed homocoupling of 1,3,5-triethylbenzene (**2**). Because **HCMP** does not contain any DMAP moieties in the framework, the control experiment (Table 1, entry 5) with **HCMP** demonstrates that the **DMAP-NCP** catalyst decisively contributes to the catalytic acylation reaction (Table 1, entries 1–4).
- [36] L. Shi, X. W. Wang, C. A. Sandoval, Z. Wang, H. J. Li, J. Wu, L. T. Yu, K. L. Ding, *Chem. Eur. J.* **2009**, *15*, 9855–9867.

Received: September 27, 2011

Revised: January 21, 2012

Published online: March 29, 2012